



# Fuzzy mathematical morphology for color images defined by fuzzy preference relations



Agustina Bouchet<sup>a,b</sup>, Pedro Alonso<sup>c</sup>, Juan Ignacio Pastore<sup>a,b</sup>, Susana Montes<sup>d</sup>, Irene Díaz<sup>e,\*</sup>

<sup>a</sup> Digital Image Processing Lab, ICyTE, Engineering Faculty National University of Mar del Plata, Argentina

<sup>b</sup> CONICET, Argentina

<sup>c</sup> Department of Mathematics, University of Oviedo, Spain

<sup>d</sup> Department of Statistics and O.R., University of Oviedo, Spain

<sup>e</sup> Department of Computer Science, University of Oviedo, Spain

## ARTICLE INFO

### Article history:

Received 2 July 2015

Received in revised form

25 May 2016

Accepted 17 June 2016

Available online 27 June 2016

### Keywords:

Mathematical Morphology

Color Images

Morphological Operators

Fuzzy Order

Fuzzy Preference Relations

## ABSTRACT

Nowadays, the representation and the treatment of color images are still open problems. Mathematical morphology is the natural area for a rigorous formulation of many problems in image analysis. Moreover, it comprises powerful non-linear techniques for filtering, texture analysis, shape analysis, edge detection or segmentation. A large number of morphological operators have been widely defined and tested to process binary and gray scale images. However, the extension of mathematical morphology operators to multi-valued functions, and in particular to color images, is neither direct nor general due to the vectorial nature of the data. In this paper, basic morphological operators, erosion and dilation, are extended to color images from a new vector ordering scheme based on a fuzzy order in the RGB color space. Experimental results show that the proposed color operators can be efficiently used for color image processing.

© 2016 Elsevier Ltd. All rights reserved.

## 1. Introduction

Techniques of artificial vision have been initially developed for binary and gray scale images, where the information is codified by 2 and  $2^{n+1}$  with  $n \in \mathbb{N}$  levels respectively. Nevertheless, the color is an important source of information. For this reason, during the last years these techniques have been developed for color images. However, nowadays, the representation and the treatment of color images are still open problems [1–4].

Mathematical morphology is the natural area for a rigorous formulation of many problems in image analysis, as well as a powerful non-linear technique which includes operators for the filtering, texture analysis, shape analysis, edge detection or segmentation. In the 1980s, Matheron and Serra [5–8] proposed the last mathematical formulation of morphology within the algebraic framework of the lattices. This means that the definition of morphological operators needs a totally ordered complete lattice structure. In that context, before defining the basic morphological operators (erosion and dilation) it is necessary to define an order on the space used for processing the images.

\* Corresponding author.

E-mail addresses: [abouchet@fi.mdp.edu.ar](mailto:abouchet@fi.mdp.edu.ar) (A. Bouchet), [palonso@uniovi.es](mailto:palonso@uniovi.es) (P. Alonso), [jpastore@fi.mdp.edu.ar](mailto:jpastore@fi.mdp.edu.ar) (J.I. Pastore), [montes@uniovi.es](mailto:montes@uniovi.es) (S. Montes), [sirene@uniovi.es](mailto:sirene@uniovi.es) (I. Díaz).

The definition of an order for both binary and gray levels images is straightforward because for both sets an order relation exists, inclusion for binary images and the order relation inherited from  $\mathbb{R}$  for gray levels image. However, for color images two problems arise. On one hand, the chromatic space in which the image is processed [9,10]. On the other hand, it is not clear what order is the best because of the vectorial nature of the data [11–19]. Barnett [20] introduced four types of vector orderings: marginal (M-order), reduced (R-order), conditional (C-order) and partial (P-order). When applied to color data, all these orderings have certain disadvantages, depending on the goal. For instance, the marginal ordering introduces false colors [16,21,22] and the conditional ordering generates visual nonlinearities from the human perception point of view; the reduced and partial orderings are either relying on pre-orderings, thus lacking the anti-symmetry property, or generate perceptual nonlinearities, as conditional orderings.

A widely used order in the literature is the lexicographic one. Several authors have used the complete lattice associated to this order and defined the dilation and erosion operators for color images according to it [1,10–12,18,21]. Although the results based on it are successful, this order is not suitable because some component is more important than the others when vectors are sorted. Therefore, it is necessary to make a choice in advance and therefore the component selected as priority will have more weight

than the others, so that the order will depend on this choice. This is an important drawback because in many problems all the components must have the same importance.

The starting point of this paper is fuzzy mathematical morphology. It is a different approach extension of the mathematical morphology's binary operators to gray level images, by redefining the set operations as fuzzy set operations. It is based on fuzzy sets theory [23–30]. The goal of this paper is to define the operators of the fuzzy mathematical morphology for color images through the use of a fuzzy order. In addition, the extended operators consider all the components with the same weight and avoid false colors.

Note that this approach could be applied to other multivariate images. However, the extension of mathematical morphological operators to multichannel data with hundreds of spectral channels is not straightforward. Some interesting results about ordering for multivariate images in high dimensional spaces can be found in [31–33]. The approach proposed in [31] consists in computing an order based on the distance to a central value, obtained by the statistical depth function, while in [32] an additive morphological decomposition based on morphological operators is considered. On the other hand, in [33], the authors presented different kinds of partial orders based on the end member representation of the hyperspectral images.

This paper is organized as follows: Section 2 reviews the general concepts of the mathematical morphology for color images; Section 3 presents the main contribution of this paper, i.e., a fuzzy ordering based on preference relations. Besides, the way in which the fuzzy order is applied to color images is explained. Section 4 studies invariant properties. In Section 5 the results obtained with the fuzzy mathematical morphology for some color images are shown. Finally, the last section details some conclusions and discusses possible future lines of research.

## 2. Mathematical morphology for color images

Mathematical morphology (MM) is a non-linear theory for spatial analysis of images where the topological relations and the geometry of the objects in the image are the parameters characterizing the object under study [5–7,34]. The main idea of this methodology is the decomposition of an operator into a combination of the basic operators: erosion, dilation, anti-erosion and anti-dilation, as well as the supreme and the infimum operations.

Fuzzy set theory has been extensively applied to image processing [27]. In particular, one extension of binary MM is the fuzzy mathematical morphology (FMM) [23,24,27–30,35]. It incorporates fuzzy logic concepts for extending binary morphological operators to gray levels images allowing us to model and manipulate in a different way the uncertainty and imprecision present almost in all different types of images. One possible approach is to fuzzify the logical operators involved in the intersection and inclusion definitions required to define dilation and erosion [23,24]. In the same line in [27] fuzzy dilation and fuzzy erosion is presented a similar approach but  $t$ -norms are used instead of a conjunctive to define the fuzzy dilation and the associated model implicator to define the fuzzy erosion. This model is less general than the previous one. Extending the Minkowski addition to an operation on fuzzy sets in  $\mathbb{R}^n$  is another possibility to define a fuzzy dilation [24]. There are also other different approaches as those based on non-fault operators [36].

The afore mentioned approaches extend the initial basic morphological operators defined for sets (binary images) in an immediate way to functions (gray levels images) [5–7,34,37]. This extension was made in a natural way because in both sets exist an

order relation, inclusion for binary images and the order relation inherited from  $\mathbb{R}$  in the case of gray level images. Therefore, the complete lattice can integrate the theoretical models of the MM. Assuming this, the color mathematical morphology (CMM) can be developed from the MM for gray level images. In that case, the definition of a complete lattice in the color space representing the chromatic information of the digital images becomes necessary. However, there is not a natural order for multidimensional data and therefore the extension of MM to CMM is not straightforward.

This will be our starting point for processing color images. Analogously to CMM, the FMM for color images is developed from the definition of a total fuzzy order.

The morphological processing of color images, modeled as functions  $f: D_f \subset \mathbb{R}^2 \rightarrow \tau \subset \mathbb{R}^3$  ( $D_f$  is the domain of the image and  $\tau$  represents the color space) is usually performed from two points of view: the marginal processing and the vectorial processing [13].

The marginal processing consists in applying the morphological operators defined for gray scale images to each color component of the image. An important drawback of this approach is that false colors usually appear as the combination of the processing components that generate new sequences of pixels. Actually this is an important problem that should be avoided. The vectorial processing is based on applying a unique operation to the image considering it as an indivisible composition of vectorial pixels. In such approach the notion of a complete lattice arises and therefore the definition of a total order over the subset  $\tau$  of  $\mathbb{R}^3$  becomes necessary. Since there is not any natural order in these sets, it is necessary to establish an appropriate order on color space  $\tau$ .

As marginal processing is a particular case of vectorial processing, once the order is defined, it is possible to provide a general definition for the basic operators called erosion and dilation (see Section 2.2). Previously, it is necessary to introduce the concept of a structuring element.

### 2.1. Structuring element

MM examines the geometrical structures of the image by checking a small neighborhood, called structuring elements (SEs), in different parts of the image. The SE is a completely defined set whose geometry is known in advance. It is compared to the image through translations. The size and shape of the SEs are chosen a priori depending on the morphology of the set over which it interacts and also according to the desired shape extraction. The SEs are then moved, so that they cover the whole image pixel by pixel, making a comparison between each element and the image.

To define the operators of the CMM, the SE plays an important role. In this case, the SE is not a set as in the binary case or a function as in the case of gray levels images, but it indicates the neighborhood over which the pixels of the image are compared.

**Definition 1.** Let  $f: D_f \subset \mathbb{R}^2 \rightarrow \mathbb{R}^3$  be a color image, let  $x \in D_f$  be a pixel, and let  $(D_f, d)$  be a metric space. A *structuring element* (SE for short) for a color pixel  $x$  is a neighborhood:

$$B(x, r) = \{y \in D_f: d(x, y) \leq r\} \quad (1)$$

where  $r$  denotes any positive real number, which is called *diameter*.

**Remark 2.** The function  $d$  is a metric or distance function on  $D_f$ , that is, for any  $x, y, z \in D_f$ ,  $d$  satisfies the following properties:

- i.  $d(x, y) \geq 0$ ,
- ii.  $d(x, y) = 0 \Leftrightarrow x = y$ ,
- iii.  $d(x, y) = d(y, x)$ ,
- iv.  $d(x, y) \leq d(x, z) + d(z, y)$ .

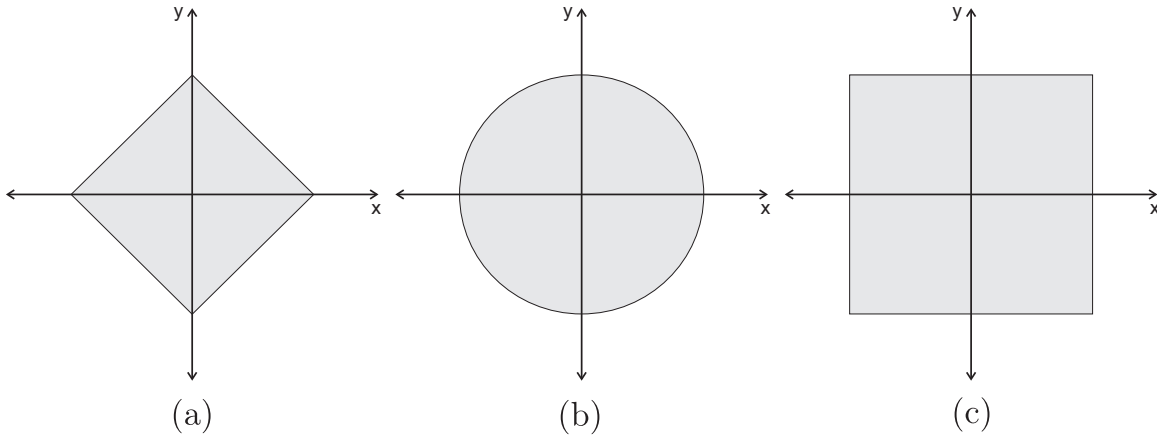


Fig. 1. Different structuring elements: (a) SE defined by  $d_1$ . (b) SE defined by  $d_2$ . (c) SE defined by  $d_\infty$ .

Basic examples of different neighborhoods are presented below. They coincide with the notion of SE, which is completely defined by considering  $D_f \subset \mathbb{R}^2$ ,  $x = (x_1, x_2)$ ,  $y = (y_1, y_2) \in D_f$  with one of the following metrics:

- (a) Manhattan distance:  $d_1(x, y) = \sum_{i=1}^2 |x_i - y_i|$
- (b) Euclidean distance:  $d_2(x, y) = \left[ \sum_{i=1}^2 (x_i - y_i)^2 \right]^{1/2}$
- (c) Infinity distance:  $d_\infty(x, y) = \max_{1 \leq i \leq 2} |x_i - y_i|$

Fig. 1 shows the SEs induced by the previous distances. The geometry and the connectivity of the neighborhood of a pixel are defined by the used metric while the dimension is defined by the diameter of the neighborhood.

2.2. Erosion and dilation for color images

As it was previously mentioned, the definition of the basic operators requires a complete lattice in the color image space. This complete lattice depends on an order between images, based on an order on  $\mathbb{R}^3$ . It is defined as follows:

**Proposition 3 ([7]).** Let  $\leq_\tau$  be an order on  $\tau \subset \mathbb{R}^3$ . The space of functions from  $D_f$  to  $\tau$  with the order  $\leq$  defined as

$$f \leq g \Leftrightarrow f(x) \leq_\tau g(x), \quad \forall x \in D_f$$

for any  $f, g: D_f \subseteq \mathbb{R}^2 \rightarrow \tau \subseteq \mathbb{R}^3$  has a lattice structure.

The basic operators for color images are now introduced.

**Definition 4.** Let  $\tau \subset \mathbb{R}^3$  be a color space with a structure of complete lattice provided by a total order  $\leq_\tau$ . Let  $B$  be a SE, the basic operators *erosion* ( $\epsilon_B^{\leq_\tau}$ ) and *dilation* ( $\delta_B^{\leq_\tau}$ ) associated to a color image  $f$  are defined as follows:

$$\epsilon_B^{\leq_\tau}(f) = \inf_{x \in B} \{f \circ T_x\} \tag{2}$$

$$\delta_B^{\leq_\tau}(f) = \sup_{x \in B} \{f \circ T_x\} \tag{3}$$

being  $T_x: \mathbb{R}^2 \rightarrow \mathbb{R}^2$  the translation function by the element  $x \in \mathbb{R}^2$ , that is,  $T_x(s) = s + x$ .

Note that for any color image  $f$ , any erosion  $\epsilon_B^{\leq_\tau}(f)$  and any dilation  $\delta_B^{\leq_\tau}(f)$  are new color images.

**Example 5.** Let  $f$  be a color image in RGB space,  $B$  the SE defined by  $d_\infty$  with  $r=3$  and  $x$  the central pixel of the SE. Fig. 2 shows the

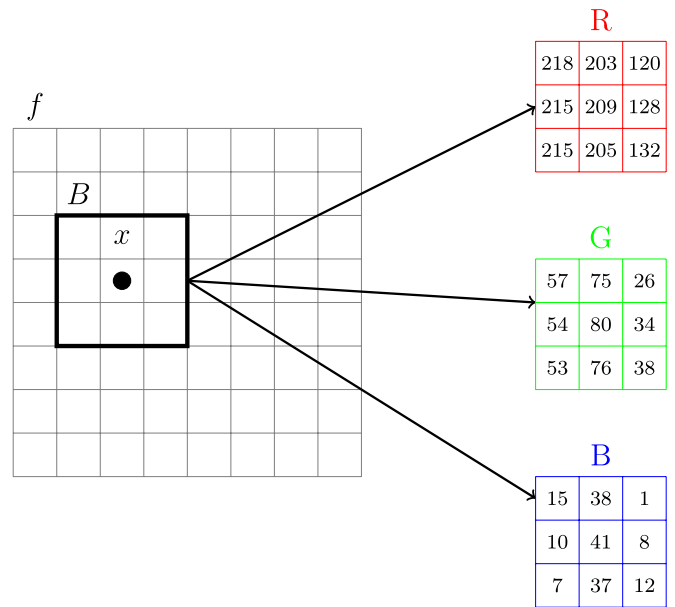


Fig. 2. Image decomposition in a neighborhood.

different objects  $f, B, x$  and the decomposition of the neighborhood defined by  $B$  in the three components of the RGB space. As an example, we take some values in each component.

Therefore, to define the erosion or dilation it is necessary to sort the pixels of the neighborhood to determine the infimum or maximum respectively. The pixels to sort are the following:  $x_1 = (218, 57, 15)$ ;  $x_2 = (215, 54, 10)$ ;  $x_3 = (215, 53, 7)$ ;  $x_4 = (203, 75, 38)$ ; ...;  $x_9 = (132, 38, 12)$  (see Fig. 2).

Applying an order to sort the pixels, both the infimum and maximum of the pixels are found. In next sections, the way proposed to order the points is explained. Assume, for example, that the infimum is  $(120, 26, 1)$ . Therefore, the central pixel of the neighborhood is replaced by this value as it is shown in Fig. 3. Following this strategy, the erosion of the color image  $f$  is obtained. Analogously we can obtain the dilation taking the maximum of the pixels.

From the combination of these basic operators, erosion and dilation, other operations can be defined in the same way they were defined for binary and gray levels images [7,34], as we can see in the following definition.

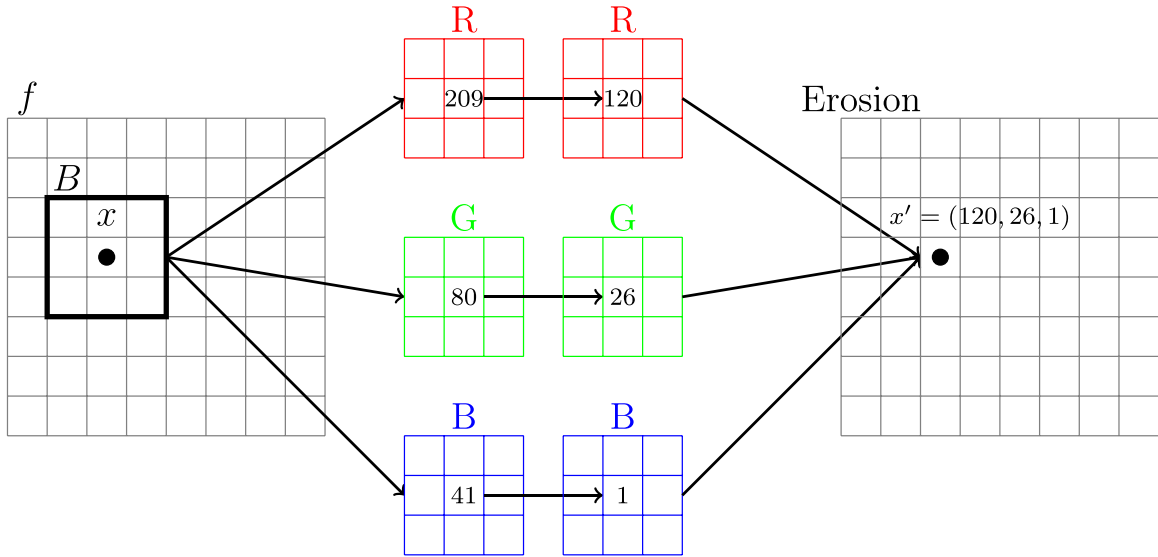


Fig. 3. Example of an erosion.

**Definition 6.** Let  $f$  a color image and  $B$  be a SE, the following morphological operators are defined as:

- Morphological gradient:
 
$$\text{Grad}_B^{\leq r}(f) = \delta_B^{\leq r}(f) - \varepsilon_B^{\leq r}(f) \quad (4)$$

- Gradient by erosion:
 
$$\text{Grad\_Ero}_B^{\leq r}(f) = f - \varepsilon_B^{\leq r}(f) \quad (5)$$

- Gradient by dilation:
 
$$\text{Grad\_Dil}_B^{\leq r}(f) = \delta_B^{\leq r}(f) - f \quad (6)$$

- Opening:
 
$$\gamma_B^{\leq r}(f) = \delta_B^{\leq r}(\varepsilon_B^{\leq r}(f)) \quad (7)$$

- Closing:
 
$$\phi_B^{\leq r}(f) = \varepsilon_B^{\leq r}(\delta_B^{\leq r}(f)) \quad (8)$$

Let us remark that the erosion and dilation of a color image strongly depend on the order established in the color space. Therefore, it has not a unique meaning as in the case of the operators of the MM for binary and gray levels images. In the following section, the order proposed for CMM is explained.

### 3. Ordering color images

This section is focused on describing the total fuzzy order proposed for comparing color structures. As a color image is represented by a vector (independently of the selected representation), it is necessary to study how to compare and order pixels.

#### 3.1. Color image representation

There are many different color representations [9]. RGB is the most straightforward representation system to manage color images, widely used in computer system and hardware devices for color image display. HLS representation system is a color image polar representation with the variables luminance, saturation and hue (lum/sat/hue). HLS systems avoids some lacks of RGB model,

but it presents some problems from the quantitative point of view [1]. There are also other representation as HSV or  $L^*a^*b^*$ . However, the choice of a suitable color space representation is still a challenging task in the processing and analysis of color images [9,38].

Thus, RGB space is chosen in this work because the three components of the image have the same nature, representing a quantity of a certain primary color. This property is not satisfied for other color spaces. RGB space is the only codification such that all the components represent the same concept, the level of saturation of a primary color. An image in this model is composed by three images, each of them corresponding with a primary color: red (R), green (G) and blue (B). One possible approach to process color images is the individual processing of these images. Using this approach, it is possible to extract shapes and significative details of the images. However, some tasks as the identification of an object and the posterior extraction of the scene can be better solved using the color as a descriptor. For this reason, it is important to process color images in the color space. On the other hand, the order proposed can be applied to any subset of  $R^n$ . This allows working with different types of multidimensional data, and thus, with different representation models [33].

A color image ordering problem is focused on looking for the pixel (among the  $n$  representing an image) which is preferred according to some criterion. This problem can be seen as a group decision problem with  $n$  alternatives (pixels in this framework)  $\mathcal{A} = \{a_1, \dots, a_n\}$ , ( $n \geq 2$ ) and 3 experts  $\mathcal{E} = \{e_1, e_2, e_3\}$  (the RGB components). Each expert (RGB component) provides his preference among the set of alternatives (pixels). The goal of the group decision making problem is to look for the alternative which is most accepted by the experts [39]. The goal here is to apply a group decision making strategy to identify the pixel most accepted according to the color representation.

In the following section, the method to select the most accepted pixel is described. The general procedure described in [40] is adapted to the pixel ordering problem.

#### 3.2. Fuzzy order

For ordering alternatives in a general framework, it is necessary to follow the next three steps [39]: Making uniform the informa-

tion, aggregating and exploiting the information. These three steps are described below for pixel ordering.

3.2.1. Making the information uniform

The first step consists in transforming each alternative into a fuzzy preference relation. Thus, a vector  $x_i = (x_i^R, x_i^G, x_i^B)$  with utility values associated to the 3 color components is associated to each pixel  $i$ . Following the method described in [40], three matrices (one associated to each different color component)  $P^k$ ,  $k = R, G, B$  are constructed as follows:

$$p_{ij}^k = h(x_i^k, x_j^k) = \frac{(x_i^k)^s}{(x_i^k)^s + (x_j^k)^s}, \quad i \neq j, \quad i, j = 1, 2, \dots, n, \tag{9}$$

where  $s$  denotes any fixed positive real number.

The structure of these matrices is given by means of the fuzzy preference relations. This well-known concept is introduced below.

**Definition 7.** Let  $\mathcal{A}$  be a finite set of alternatives, a fuzzy preference relation  $P$  is a mapping  $P: \mathcal{A} \times \mathcal{A} \rightarrow [0, 1]$  such that  $P(a, b) + P(b, a) = 1$  for each pair of alternatives  $a$  and  $b$  in  $\mathcal{A}$ . If  $\mathcal{A}$  has  $n$  elements,  $P$  can be represented as a matrix:

$$P = \begin{pmatrix} p_{11} & \dots & p_{1n} \\ \vdots & \dots & \vdots \\ p_{n1} & \dots & p_{nn} \end{pmatrix}, \tag{10}$$

where  $p_{ij} = P(a_i, a_j)$  denotes the degree to which alternative  $a_i$  is preferred to alternative  $a_j$ .

Moreover, if  $P(a, b) \in [0, 1/2)$ ,  $b$  is said to be preferred over  $a$ . If  $P(a, b) \in [1/2, 1]$ , then  $a$  is said to be preferred over  $b$ . Finally, in the case  $P(a, b) = 1/2$ ,  $a$  and  $b$  are said to be indifferent.

Thus, in the context of this work, each matrix  $P^k$  represents the fuzzy preference relations associated to one color (red, green or blue). Therefore, considering the particular framework of RGB images, a neighborhood of dimension  $n$  can be represented by its pixels as follows:

$$\begin{pmatrix} x_1^R x_1^G x_1^B \\ x_2^R x_2^G x_2^B \\ \vdots \\ x_n^R x_n^G x_n^B \end{pmatrix} \tag{11}$$

where the columns respectively correspond to the red, green and blue components. Following the procedure afore defined and considering the case  $s=1$ , the three  $n \times n$ -matrices  $P^R, P^G$  and  $P^B$  are generated as follows:

$$p_{ij}^R = \begin{cases} \frac{x_i^R}{x_i^R + x_j^R}, & \text{if } x_i^R > 0 \text{ or } x_j^R > 0, \\ 0.5 & \text{otherwise,} \end{cases} \tag{12}$$

where  $p_{ij}^R$  means the preference of red between the  $x_i$  and  $x_j$  pixels. If  $p_{ij}^R$  takes values greater than 0.5, it means that the  $x_i$  pixel is more intense in the red component than the  $x_j$  pixel. If  $p_{ij}^R$  is less than 0.5, it means that the  $x_j$  pixel is more intense in the red component than  $x_i$ . Finally, if it is equal to 0.5, that means that the red intensity of both pixels is the same.

In an equivalent way the preferences for the other components are defined.

$$p_{ij}^G = \begin{cases} \frac{x_i^G}{x_i^G + x_j^G}, & \text{if } x_i^G > 0 \text{ or } x_j^G > 0, \\ 0.5 & \text{otherwise,} \end{cases} \tag{13}$$

and

$$p_{ij}^B = \begin{cases} \frac{x_i^B}{x_i^B + x_j^B}, & \text{if } x_i^B > 0 \text{ or } x_j^B > 0, \\ 0.5 & \text{otherwise.} \end{cases} \tag{14}$$

When the two values to compare are equal to zero, the value of  $p_{ij}$  is an indetermination. To avoid this,  $p_{ij} = 0.5$  as the preference between pixels  $x_i$  and  $x_j$  is the same, i.e., they have the same intensity. This usually occurs, for example, when two pixels correspond to the background of the image. Note that the approach followed when the two values to compare are equal to zero differs from the one presented in [40].

**Example 8.** Considering the pixels provided in Example 5, the following matrix is obtained:

$$\begin{pmatrix} 218 & 57 & 15 \\ 215 & 54 & 10 \\ 215 & 53 & 7 \\ 203 & 75 & 38 \\ 209 & 80 & 41 \\ 205 & 76 & 37 \\ 120 & 26 & 1 \\ 128 & 34 & 8 \\ 132 & 38 & 12 \end{pmatrix}$$

According to formulas (12), (13) and (14) the three matrices  $P^R, P^G$  and  $P^B$  are obtained:

$$P^R = \begin{pmatrix} 0.5000 & 0.5035 & 0.5035 & 0.5178 & 0.5105 & 0.5154 & 0.6450 & 0.6301 & 0.6229 \\ 0.4965 & 0.5000 & 0.5000 & 0.5144 & 0.5071 & 0.5119 & 0.6418 & 0.6268 & 0.6196 \\ 0.4965 & 0.5000 & 0.5000 & 0.5144 & 0.5071 & 0.5119 & 0.6418 & 0.6268 & 0.6196 \\ 0.4822 & 0.4856 & 0.4856 & 0.5000 & 0.4927 & 0.4975 & 0.6285 & 0.6133 & 0.6060 \\ 0.4895 & 0.4929 & 0.4929 & 0.5073 & 0.5000 & 0.5048 & 0.6353 & 0.6202 & 0.6129 \\ 0.4846 & 0.4881 & 0.4881 & 0.5025 & 0.4952 & 0.5000 & 0.6308 & 0.6156 & 0.6083 \\ 0.3550 & 0.3582 & 0.3582 & 0.3715 & 0.3647 & 0.3692 & 0.5000 & 0.4839 & 0.4762 \\ 0.3699 & 0.3732 & 0.3732 & 0.3867 & 0.3798 & 0.3844 & 0.5161 & 0.5000 & 0.4923 \\ 0.3771 & 0.3804 & 0.3804 & 0.3940 & 0.3871 & 0.3917 & 0.5238 & 0.5077 & 0.5000 \end{pmatrix}$$

$$P^G = \begin{pmatrix} 0.5000 & 0.5135 & 0.5182 & 0.4318 & 0.4161 & 0.4286 & 0.6867 & 0.6264 & 0.6000 \\ 0.4865 & 0.5000 & 0.5047 & 0.4186 & 0.4030 & 0.4154 & 0.6750 & 0.6136 & 0.5870 \\ 0.4818 & 0.4953 & 0.5000 & 0.4141 & 0.3985 & 0.4109 & 0.6709 & 0.6092 & 0.5824 \\ 0.5682 & 0.5814 & 0.5859 & 0.5000 & 0.4839 & 0.4967 & 0.7426 & 0.6881 & 0.6637 \\ 0.5839 & 0.5970 & 0.6015 & 0.5161 & 0.5000 & 0.5128 & 0.7547 & 0.7018 & 0.6780 \\ 0.5714 & 0.5846 & 0.5891 & 0.5033 & 0.4872 & 0.5000 & 0.7451 & 0.6909 & 0.6667 \\ 0.3133 & 0.3250 & 0.3291 & 0.2574 & 0.2453 & 0.2549 & 0.5000 & 0.4333 & 0.4063 \\ 0.3736 & 0.3864 & 0.3908 & 0.3119 & 0.2982 & 0.3091 & 0.5667 & 0.5000 & 0.4722 \\ 0.4000 & 0.4130 & 0.4176 & 0.3363 & 0.3220 & 0.3333 & 0.5938 & 0.5278 & 0.5000 \end{pmatrix}$$

$$P^B = \begin{pmatrix} 0.5000 & 0.6000 & 0.6818 & 0.2830 & 0.2679 & 0.2885 & 0.9375 & 0.6522 & 0.5556 \\ 0.4000 & 0.5000 & 0.5882 & 0.2083 & 0.1961 & 0.2128 & 0.9091 & 0.5556 & 0.4545 \\ 0.3182 & 0.4118 & 0.5000 & 0.1556 & 0.1458 & 0.1591 & 0.8750 & 0.4667 & 0.3684 \\ 0.7170 & 0.7917 & 0.8444 & 0.5000 & 0.4810 & 0.5067 & 0.9744 & 0.8261 & 0.7600 \\ 0.7321 & 0.8039 & 0.8542 & 0.5190 & 0.5000 & 0.5256 & 0.9762 & 0.8367 & 0.7736 \\ 0.7115 & 0.7872 & 0.8409 & 0.4933 & 0.4744 & 0.5000 & 0.9737 & 0.8222 & 0.7551 \\ 0.0625 & 0.0909 & 0.1250 & 0.0256 & 0.0238 & 0.0263 & 0.5000 & 0.1111 & 0.0769 \\ 0.3478 & 0.4444 & 0.5333 & 0.1739 & 0.1633 & 0.1778 & 0.8889 & 0.5000 & 0.4000 \\ 0.4444 & 0.5455 & 0.6316 & 0.2400 & 0.2264 & 0.2449 & 0.9231 & 0.6000 & 0.5000 \end{pmatrix}$$

where, for example,  $p_{43}^R = \frac{203}{203 + 215} = 0.4856$ .

Once these matrices are obtained, the global preference relation is obtained by aggregating the three components following the procedure detailed in the next subsection.

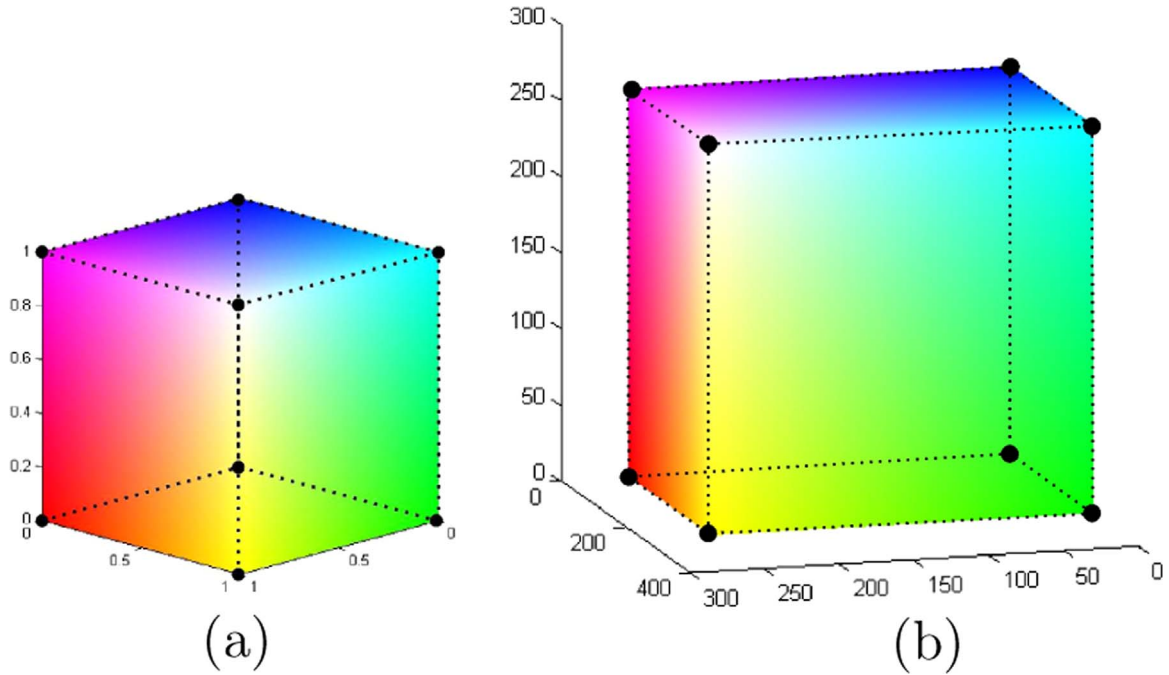


Fig. 4. Invariance properties of fuzzy order. (a) Unit cube. (b) Unit cube translate, scale and rotate.

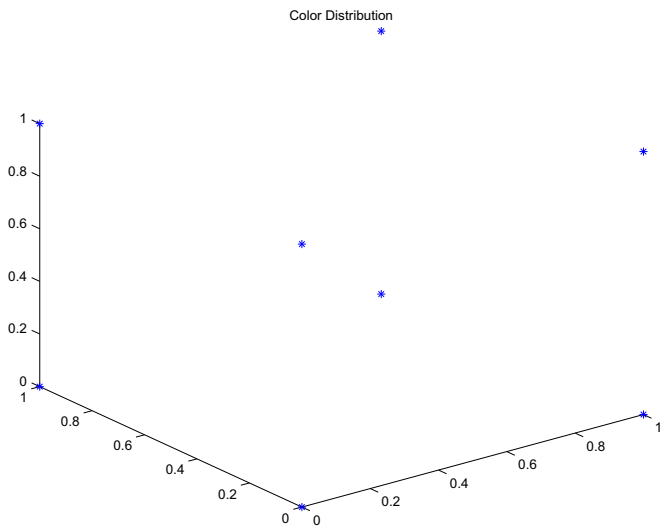


Fig. 5. Invariance properties of fuzzy order. Eight colors corresponding to the vertices of both cubes. (For interpretation of the references to color in this figure caption, the reader is referred to the web version of this paper.)

3.2.2. Aggregation step

Using the preferences associated to each color component, a consensus fuzzy preference relation is obtained using an aggregation operator. This concept is introduced in the next definition.

**Definition 9.** Let  $I$  be a closed interval in  $\mathbb{R}$ . An *ordered weighted averaging aggregation operator* (OWA for short) is any aggregation operator defined by:

$$f_{OWA}: I^m \rightarrow I$$

$$(x_1, x_2, \dots, x_m) \rightarrow \sum_{i=1}^m w_i x_{\sigma(i)} \tag{15}$$

where  $\sigma$  is the permutation that sorts the elements in the following way:  $x_{\sigma(1)} \geq x_{\sigma(2)} \geq \dots \geq x_{\sigma(m)}$  and  $\{w_i\}_{i=1}^m$  is a family of weights such that  $w_i \geq 0$  and  $\sum_{i=1}^m w_i = 1$ .

OWA operators were originally introduced by Yager [41] to provide a method for aggregating scores associated to the satisfaction of multiple criteria. Examples of OWA operators are the arithmetic or geometric means, minimum, maximum or median.

The consensus among the 3 fuzzy preference relations is reached with an OWA operator. Therefore the matrix  $P \in \mathbb{R}^{n \times n}$  is obtained as follows:

$$p_{ij} = f_{OWA}(p_{ij}^R, p_{ij}^G, p_{ij}^B) \tag{16}$$

Each element of the new preference relation,  $p_{ij}$ , represents the preference of pixel  $x_i$  over pixel  $x_j$  according to the preferences of the red, green and blue components of the  $x_i$  pixel over the  $x_j$  pixel. Thus, the pixels can be compared as follows:

**Definition 10.** Let  $x_i = (x_i^R, x_i^G, x_i^B)$  and  $x_j = (x_j^R, x_j^G, x_j^B)$  be two pixels. Let  $f_{OWA}$  be an OWA operator. Then the pixel  $x_i$  is *more intense* than the pixel  $x_j$  if  $p_{ij} > 0.5$  with:

$$p_{ij} = f_{OWA}\left(\frac{x_i^R}{x_i^R + x_j^R}, \frac{x_i^G}{x_i^G + x_j^G}, \frac{x_i^B}{x_i^B + x_j^B}\right) \tag{17}$$

When  $p_{ij}$  is exactly equal to 0.5, pixels  $x_i$  and  $x_j$  have the *same intensity*.

The arithmetic mean is used as OWA operator as the purpose of the work is to give to all the components the same importance and then to overcome the drawback of some orders used in CMM, as for example, the lexicographic order.

**Example 11.** Considering the three matrices  $P^R, P^G$  and  $P^B$  obtained in Example 8, the matrix  $P$  is obtained:

$$P = \begin{pmatrix} 0.5000 & 0.5390 & 0.5678 & 0.4109 & 0.3982 & 0.4108 & 0.7564 & 0.6362 & 0.5928 \\ 0.4610 & 0.5000 & 0.5310 & 0.3804 & 0.3687 & 0.3800 & 0.7420 & 0.5987 & 0.5537 \\ 0.4322 & 0.4690 & 0.5000 & 0.3613 & 0.3505 & 0.3606 & 0.7292 & 0.5676 & 0.5235 \\ 0.5891 & 0.6196 & 0.6387 & 0.5000 & 0.4859 & 0.5003 & 0.7818 & 0.7092 & 0.6766 \\ 0.6018 & 0.6313 & 0.6495 & 0.5141 & 0.5000 & 0.5144 & 0.7887 & 0.7196 & 0.6882 \\ 0.5892 & 0.6200 & 0.6394 & 0.4997 & 0.4856 & 0.5000 & 0.7832 & 0.7096 & 0.6767 \\ 0.2436 & 0.2580 & 0.2708 & 0.2182 & 0.2113 & 0.2168 & 0.5000 & 0.3428 & 0.3198 \\ 0.3638 & 0.4013 & 0.4324 & 0.2908 & 0.2804 & 0.2904 & 0.6572 & 0.5000 & 0.4548 \\ 0.4072 & 0.4463 & 0.4765 & 0.3234 & 0.3118 & 0.3233 & 0.6802 & 0.5452 & 0.5000 \end{pmatrix}$$

where, for example:  $p_{23} = \frac{0.5 + 0.5047 + 0.5882}{3} = 0.5310$ .

Once the preference relation matrix is obtained, the last step consists in ordering the different alternatives (that is, the pixels). The approach followed in this paper is described in the next subsection [40].

### 3.2.3. Exploitation step

This last step is in charge of selecting the most intense pixel from the consensus fuzzy preference relation. To avoid the previous preference relation to be cyclic, an extension of the weighted voting method (EWVM) [42] is used. EWVM defines a parameter  $\alpha$  allowing to model the importance of “being desirable” or “not being preferred” among the whole pixel set.

The algorithm, proposed in [40], is described below. Taking as input a fuzzy preference relation  $P$  over a set of pixels  $\mathcal{A} = \{a_1, \dots, a_n\}$ , the parameter  $\alpha \in [0, 1]$  and an aggregation operator  $\text{Agg}$ , the method obtains a total fuzzy order among the pixels after following the steps:

1. Normalize  $P$
2. Separate the “positive preference” ( $P^+$ ) and the “negative preference” ( $P^-$ )
  - $p_{ij}^+ = \max\{0, p_{ij} - 0.5\}$
  - $p_{ij}^- = \min\{0, p_{ij} - 0.5\}$
3.  $P^\alpha = \alpha \cdot P^+ + (1 - \alpha) \cdot P^-$
4. Aggregate each row of  $P^\alpha$  and order according the aggregated value

The computational cost in flops associated to each step is also analyzed. Regarding the first step (making uniform the information), each matrix element is obtained with one addition and one division. Thus,  $3n^2$  additions and divisions are required, being  $n$  the number of

matrix elements. Thus, this is a  $O(n^2)$  step. In the aggregation step, each element is obtained with 2 additions and 1 division, that means,  $3n^2$  basic operations ( $O(n^2)$ ). Finally, in exploitation step, the most consuming task is also  $O(n^2)$ .

For more information about this method and how it performs, authors refer to [39,40]. Note that the previous algorithm induces the following total fuzzy order:

**Definition 12 ([40]).** For each set of alternatives  $\mathcal{A} = \{a_1, \dots, a_n\}$  the binary relations  $>$ ,  $\geq$  and  $\sim$  are defined as follows:

- $a_i > a_j \Leftrightarrow \exists \mathcal{K}_s, \mathcal{K}_t$  such that  $a_i \in \mathcal{K}_s, a_j \in \mathcal{K}_t$  and  $s < t$ .
- $a_i \sim a_j \Leftrightarrow \exists \mathcal{K}_s$  such that  $a_i \in \mathcal{K}_s, a_j \in \mathcal{K}_s$ .
- $a_i \geq a_j \Leftrightarrow a_i > a_j$  or  $a_i \sim a_j$ .

The binary relation  $\geq$  is called *fuzzy order*.

The name of fuzzy order is appropriate since it was proven in [40] that it is a total order and it is based on a fuzzy relation, in particular in a fuzzy preference relation.

For explaining these steps in terms of images, it is important to describe the second and the third steps of the algorithm. The second one means that preferences  $p_{ij}$  are divided into two matrices. Given  $P^+$ , each  $p_{ij}^+ > 0$  means pixel  $x_i$  is *more intense* than  $x_j$ , and the matrix  $P^-$  contains all the pixels in which  $x_j$  is *more intense* than  $x_i$ . Then, these matrices are mixed generating  $P^\alpha$ . In our case, we have considered the case  $\alpha = 0.5$  since we need all the preferences to have the same importance. Finally, the operator  $\text{Agg}$  is applied for sorting the pixels. Thus, we obtain the ordering of the pixels of the neighborhood taken in the color image.

**Example 13.** Consider the matrix  $P$  obtained in Example 11, according to Step 2 of the algorithm, we separate the pixels in which  $x_i$  is *more intense* than  $x_j$ :

$$P^+ = \begin{pmatrix} 0 & 0.0390 & 0.0678 & 0 & 0 & 0 & 0.2564 & 0.1362 & 0.0928 \\ 0 & 0 & 0.0310 & 0 & 0 & 0 & 0.2420 & 0.0987 & 0.0537 \\ 0 & 0 & 0 & 0 & 0 & 0 & 0.2292 & 0.0676 & 0.0235 \\ 0.0891 & 0.1196 & 0.1387 & 0 & 0 & 0.0003 & 0.2818 & 0.2092 & 0.1766 \\ 0.1018 & 0.1313 & 0.1495 & 0.0141 & 0 & 0.0144 & 0.2887 & 0.2196 & 0.1882 \\ 0.0892 & 0.1200 & 0.1394 & 0 & 0 & 0 & 0.2832 & 0.2096 & 0.1767 \\ 0 & 0 & 0 & 0 & 0 & 0 & 0 & 0 & 0 \\ 0 & 0 & 0 & 0 & 0 & 0 & 0.1572 & 0 & 0 \\ 0 & 0 & 0 & 0 & 0 & 0 & 0.1802 & 0.0452 & 0 \end{pmatrix}$$

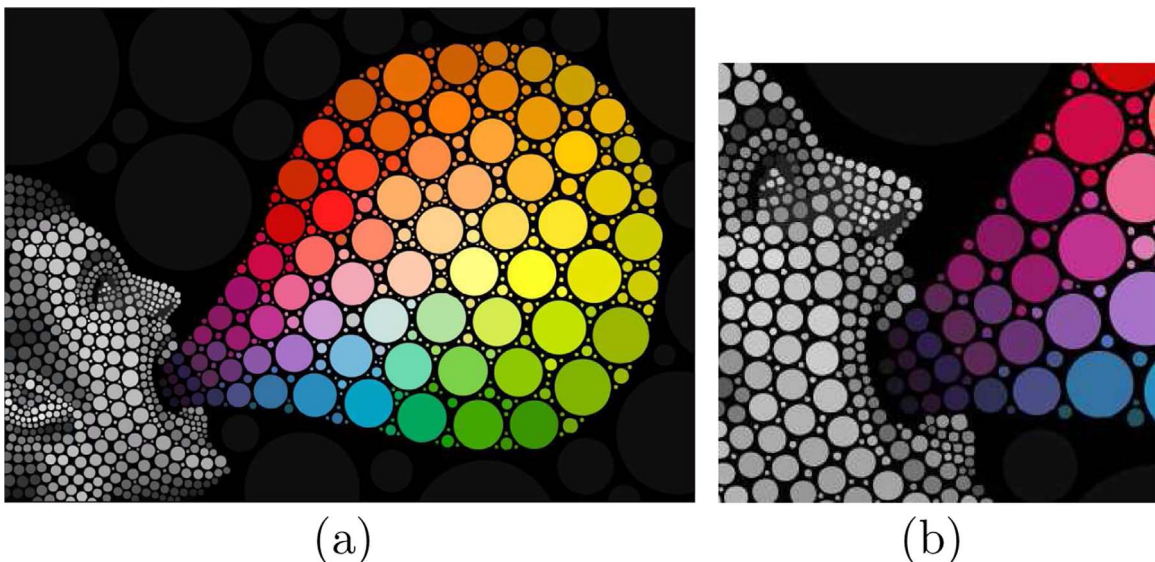


**Fig. 6.** Two synthetic image containing colored balls. (a) Original synthetic image. (b) Sub-image obtained by selecting only some pixels of (a). (For interpretation of the references to color in this figure caption, the reader is referred to the web version of this paper.)

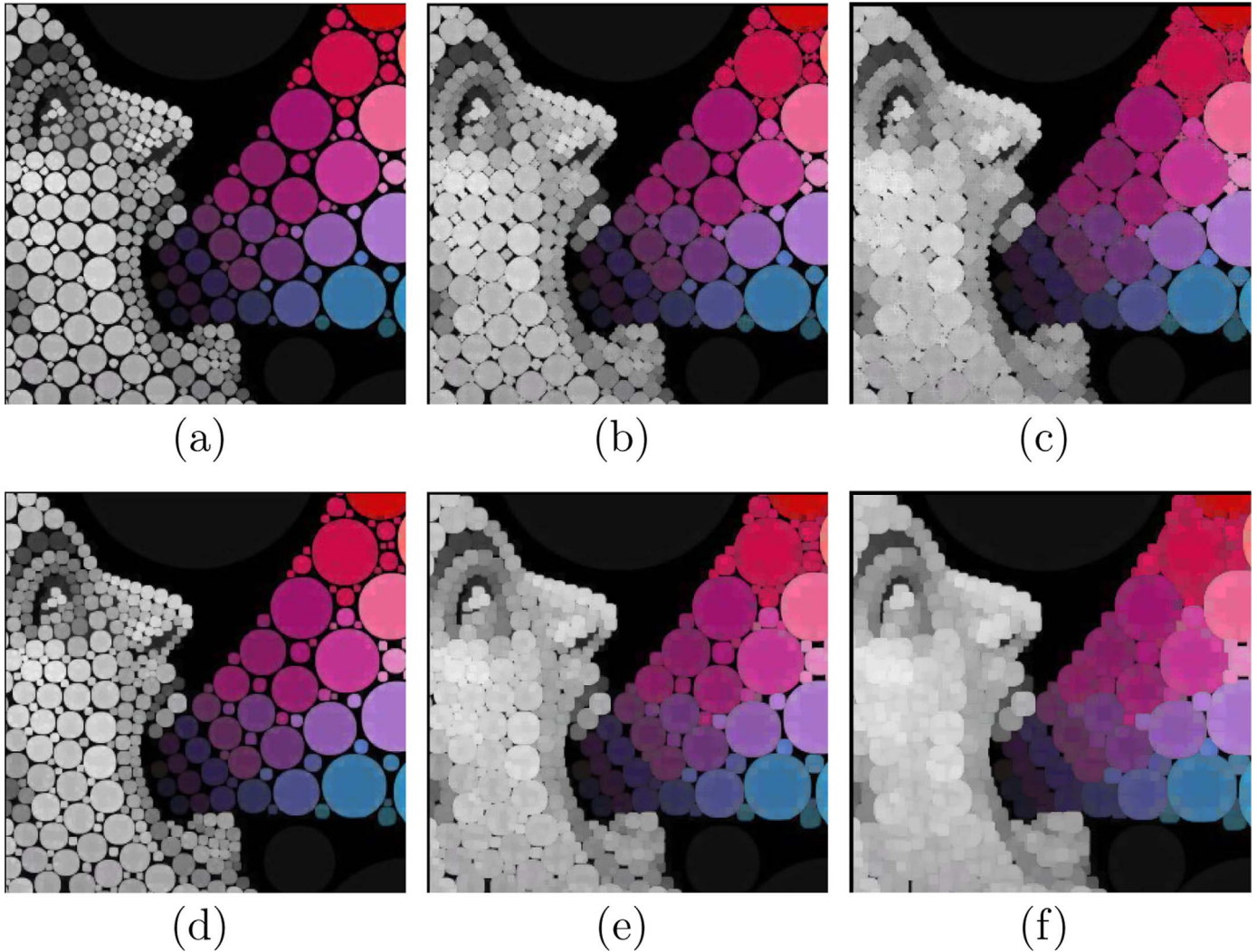


Fig. 7. Dilation obtained by  $d_1$  with (a)  $r=3$ , (b)  $r=5$ , (c)  $r=7$  and by  $d_\infty$  when (d)  $r=3$ , (e)  $r=5$ , (f)  $r=7$ .

For example in the matrix above, pixel  $x_1$  is more intense than pixel  $x_2$ . In a similar way, we separate the pixels in which  $x_j$  is more intense than  $x_i$ :

$$P^- = \begin{pmatrix} 0 & 0 & 0 & -0.0891 & -0.1018 & -0.0892 & 0 & 0 & 0 \\ -0.0390 & 0 & 0 & -0.1196 & -0.1313 & -0.1200 & 0 & 0 & 0 \\ -0.0678 & -0.0310 & 0 & -0.1387 & -0.1495 & -0.1394 & 0 & 0 & 0 \\ 0 & 0 & 0 & 0 & -0.0141 & 0 & 0 & 0 & 0 \\ 0 & 0 & 0 & 0 & 0 & 0 & 0 & 0 & 0 \\ 0 & 0 & 0 & -0.0003 & -0.0144 & 0 & 0 & 0 & 0 \\ -0.2564 & -0.2420 & -0.2292 & -0.2818 & -0.2887 & -0.2832 & 0 & -0.1572 & -0.1802 \\ -0.1362 & -0.0987 & -0.0676 & -0.2092 & -0.2196 & -0.2096 & 0 & 0 & -0.0452 \\ -0.0928 & -0.0537 & -0.0235 & -0.1766 & -0.1882 & -0.1767 & 0 & 0 & 0 \end{pmatrix}$$

Then, considering  $\alpha = 0.5$  and applying Step 3 of the algorithm, the matrix  $P^\alpha = \alpha \cdot P^+ + (1 - \alpha) \cdot P^-$  is:

$$P^\alpha = \begin{pmatrix} 0 & 0.0195 & 0.0339 & -0.0446 & -0.0509 & -0.0446 & 0.1282 & 0.0681 & 0.0464 \\ -0.0195 & 0 & 0.0155 & -0.0598 & -0.0656 & -0.0600 & 0.1210 & 0.0493 & 0.0268 \\ -0.0339 & -0.0155 & 0 & -0.0693 & -0.0748 & -0.0697 & 0.1146 & 0.0338 & 0.0117 \\ 0.0446 & 0.0598 & 0.0693 & 0 & -0.0071 & 0.0002 & 0.1409 & 0.1046 & 0.0883 \\ 0.0509 & 0.0656 & 0.0748 & 0.0071 & 0 & 0.0072 & 0.1444 & 0.1098 & 0.0941 \\ 0.0446 & 0.0600 & 0.0697 & -0.0002 & -0.0072 & 0 & 0.1416 & 0.1048 & 0.0883 \\ -0.1282 & -0.1210 & -0.1146 & -0.1409 & -0.1444 & -0.1416 & 0 & -0.0786 & -0.0901 \\ -0.0681 & -0.0493 & -0.0338 & -0.1046 & -0.1098 & -0.1048 & 0.0786 & 0 & -0.0226 \\ -0.0464 & -0.0268 & -0.0117 & -0.0883 & -0.0941 & -0.0883 & 0.0901 & 0.0226 & 0 \end{pmatrix}$$

Finally, Step 4 is applied. The Agg operator (the arithmetic mean in this case) is applied, obtaining:

$$\begin{aligned} \text{Agg}_{j=1}^9(P^\alpha(1, j)) &= 0.0173 & \text{Agg}_{j=1}^9(P^\alpha(2, j)) &= 0.0009 & \text{Agg}_{j=1}^9(P^\alpha(3, j)) &= -0.0115 \\ \text{Agg}_{j=1}^9(P^\alpha(4, j)) &= 0.0556 & \text{Agg}_{j=1}^9(P^\alpha(5, j)) &= 0.0615 & \text{Agg}_{j=1}^9(P^\alpha(6, j)) &= 0.0557 \\ \text{Agg}_{j=1}^9(P^\alpha(7, j)) &= 0.1066 & \text{Agg}_{j=1}^9(P^\alpha(8, j)) &= -0.0460 & \text{Agg}_{j=1}^9(P^\alpha(9, j)) &= -0.0270 \end{aligned}$$

Therefore, the more intense pixel is  $x_5 = (209, 80, 41)$  as the aggregated value obtained for  $x_5$  is the greater. Now  $x_5$  is deleted and the procedure is applied again to all the pixels except  $x_5$ . Repeating the process until the pixel set is empty the order of all the pixels is obtained.

#### 4. Invariant properties

In this section the invariant properties of the previously defined operators are studied according to [43]. Note that an operator  $\phi: \tau \rightarrow \tau$  is called invariant to a transformation  $\psi: \tau \rightarrow \tau$  if  $\phi(\psi(f)) = \psi(\phi(f))$ .

The method proposed in this work is clearly invariant to band permutation. In contrast, the operators defined over the lattice induced by the lexicographic order do not satisfy this important property because in this order some components of the image are prioritized over the others (see [9]).

When erosions and dilations are defined using lattice theory, erosions are operators that commute with taking the meet while dilations are operators that commute with taking the join. As the

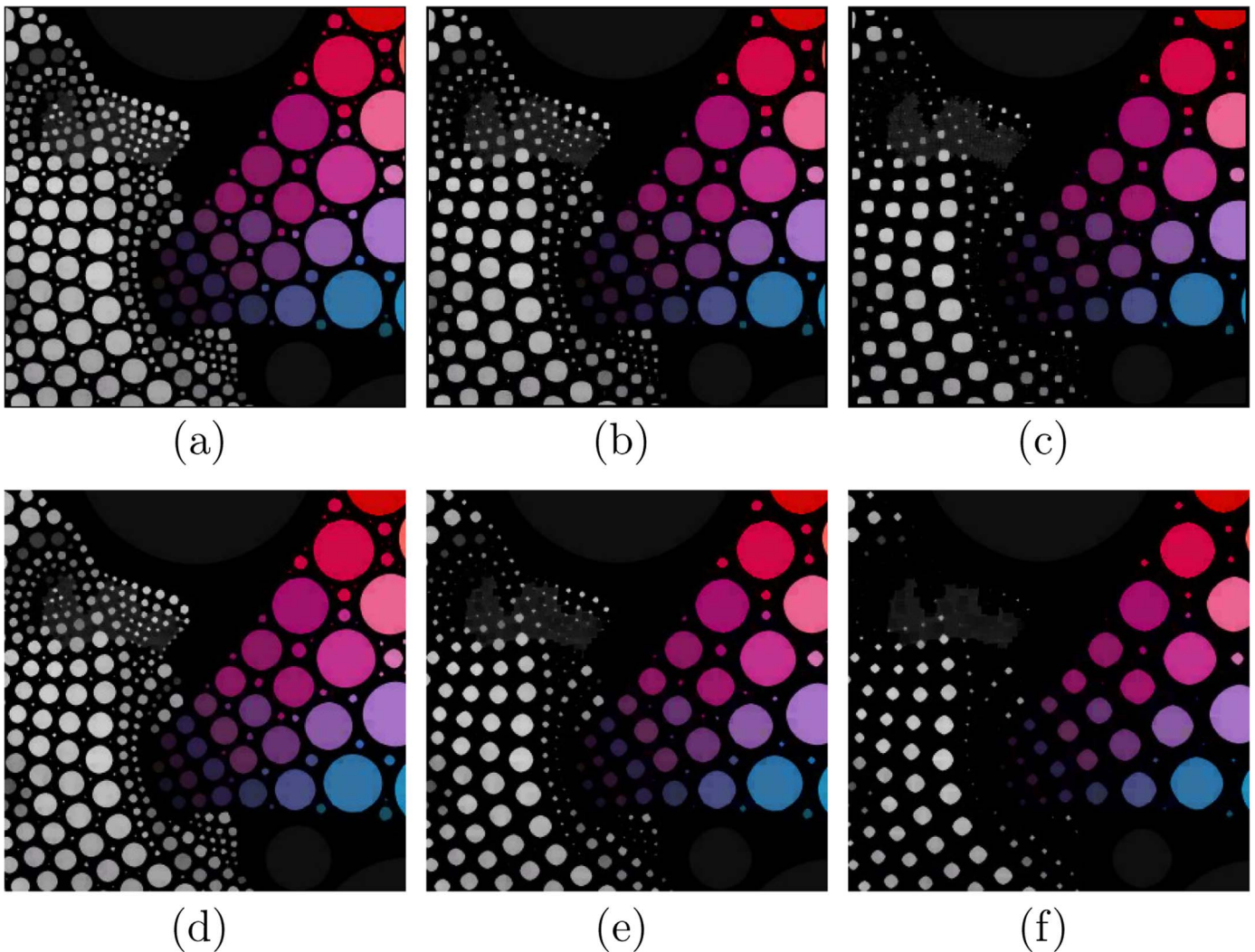


**Fig. 8.** Erosion obtained by  $d_1$  with (a)  $r=3$ , (b)  $r=5$ , (c)  $r=7$  and by  $d_\infty$  when (d)  $r=3$ , (e)  $r=5$ , (f)  $r=7$ .

fuzzy order presented in the previous section defines a complete lattice (see Definition 12), the erosion  $\epsilon_b^{\leq r}$  and the dilation  $\delta_b^{\leq r}$  are invariant with meet and join respectively.

In the same way, openings are order-preserving, anti-extensive and idempotent operators. Closings are operators that are order-preserving, extensive and idempotent. The morphological gradient  $Grad_b^{\leq r}$  is invariant under translation and scale changes.

On the other hand, an operator on a lattice  $\tau$ , or the lattice itself, is said to be invariant to a transformation group  $\mathbb{T}$  if it is invariant to all group actions in  $\mathbb{T}$ . In [7] it is proved that when erosion and dilation are defined on lattices then, they are invariant with regard to the following three transformation groups  $\mathbb{T}$ :

- Translation group formed by translation (with the null vector as a identity element).
- Translation group formed by all rotations around the gray axis (with the rotation by  $0^\circ$  as a identity element).
- Translation group formed by the change of scale (with the null vector and  $\lambda = 1$  as a identity element).

Therefore, as the erosion  $\epsilon_b^{\leq r}$  and dilation  $\delta_b^{\leq r}$  defined in this work for color images are defined using lattices, it is possible to conclude (using the results shown in [7]) that they are invariant with regard to these three transformation groups in  $\mathbb{T}$ . Fig. 4 (a) shows the unit cube. Their translation in a direction  $T_x$  and  $T_y$ ,

scaled by a parameter  $\lambda$  and rotated by an angle  $\theta$  is shown in Fig. 4(b).

Without loss of generality, the eight colors corresponding to the vertices of the unit cube are considered:

$$\epsilon = \{(0, 0, 0); (1, 0, 0); (0, 1, 0); (0, 0, 1); (1, 1, 0); (0, 1, 1); (1, 0, 1); (1, 1, 1)\}.$$

As the geometric transformations mapped the pixel coordinates  $(x, y)$  into  $(x', y')$ , without changing the color at that pixel, then these same colors correspond to the ends of the translated, scaled and rotated cube (see Fig. 5). Therefore, the infimum and supreme are given by the fuzzy order introduced in this paper. As it can be easily checked,  $\inf^{\leq r} \epsilon = (0, 0, 0)$  and  $\sup^{\leq r} \epsilon = (1, 1, 1)$ .

In next section the results obtained when this order is considered to construct the morphological operators in real images are presented.

## 5. Results

In this section some experiments are conducted to check the performance of the proposed morphological operators.

To test the method several experiments are performed. First the effect of different SE in dilation and erosion is studied.

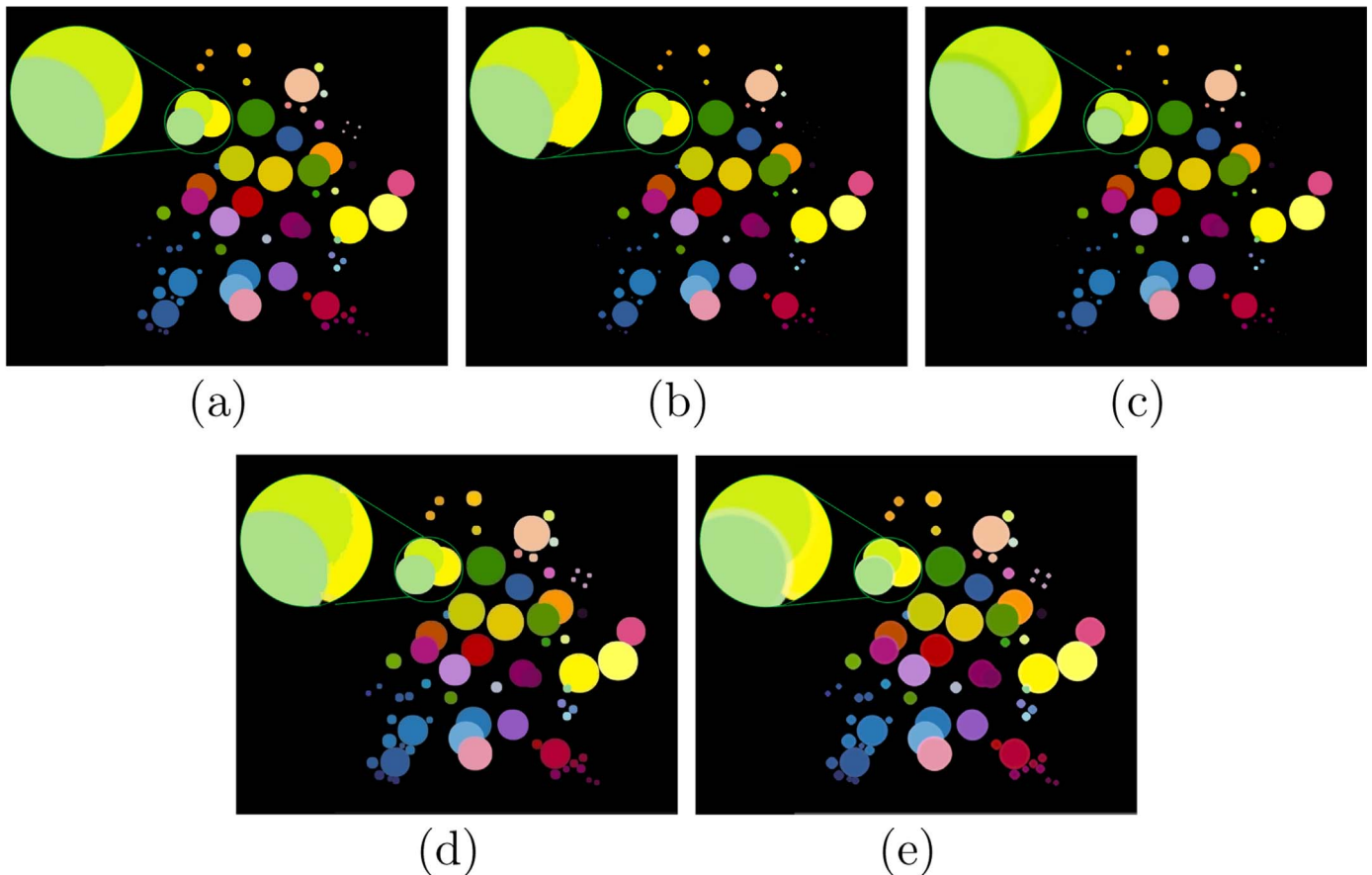


**Fig. 9.** Comparison between fuzzy and M-order using a synthetic image containing colored balls. (a) Original synthetic image. (b) Erosion with fuzzy order. (c) Erosion with M-order. (d) Dilation with fuzzy order. (e) Dilation with M-order. (For interpretation of the references to color in this figure caption, the reader is referred to the web version of this paper.)

Fig. 6 shows the images used to check the performance of the approach presented in this paper. The original image is shown in Fig. 6(a) (authored by Heine [44]). It is composed of regions where some pixels take gray level values and another pixels take colors. The test is restricted to the bounded region of the original image (Fig. 6(b)) to simplify calculations.

It is important to highlight that both color image erosion and dilation strongly depend on the order established in the color space. Therefore, it has not a unique meaning as in the case of binary images and gray levels. Figs. 7 and 8 show the behavior of  $d_1$  and  $d_\infty$  distances when  $r = 3, 5, 7$ . From this image, that combines color and gray levels, it is possible to observe that the behavior of the operators defined from fuzzy order on the gray levels are as expected. The eroded image is a darker image while the dilated image is clearer, observing the same effect on the part of color. Finally, it is observed that the shape (given by the metric) and the size (given by  $r$ ) of the structuring element determine the structure of the transformed image.

Next experiment is focused on comparing the proposed method to other two approaches, one of them based in the use of a M-order (marginal processing) and the other based in the lexicographic order. As it has been just evidenced, different metrics and diameters defined by different SEs produce diverse dilations and erosions. The selection of the SE depends on the analysis required by the problem to solve. In this case, to evidence and compare the effects of the basic operators, erosion and dilation, the SE is fixed. In particular, SE is defined by the metric  $d_\infty$  with  $r=5$ .

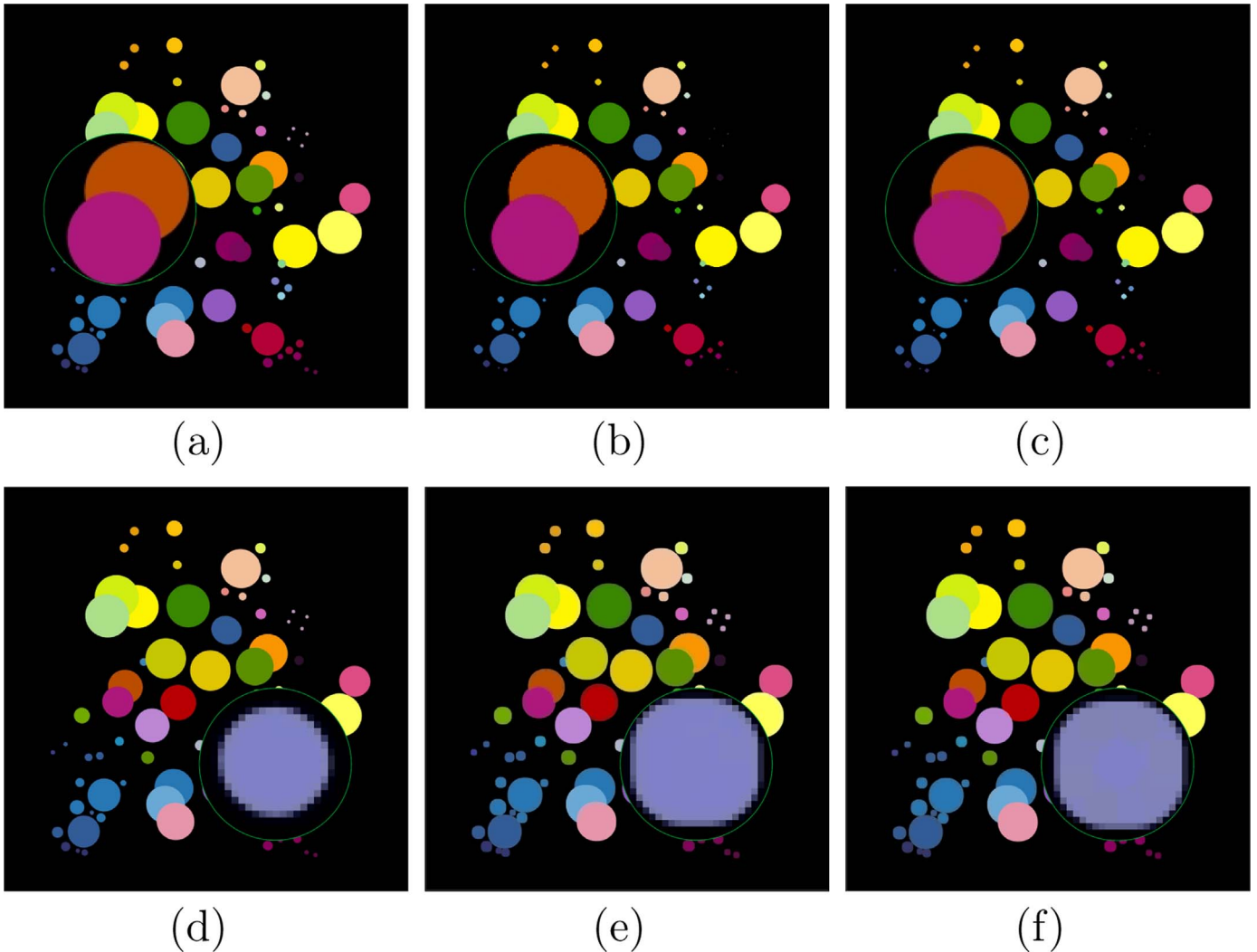
Fig. 9 shows the comparison between M-order and the approach proposed in this work when both are applied to Fig. 9(a). In the figures a region of the same image was scaled in order to

better appreciate the effects of the different operators (image (a)). Images (b) and (c) in Fig. 9 respectively represent the image (a) after erosion with fuzzy and lexicographical orders. On the other hand images (d) and (e) in Fig. 9 respectively represent the image (a) after dilation with fuzzy and lexicographical orders.

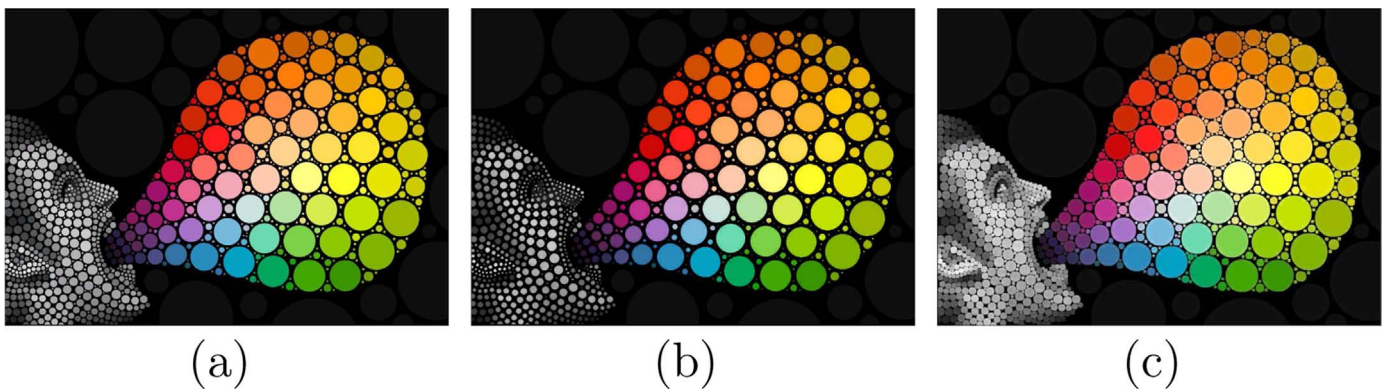
As it can be observed when applying M-order false colors appear as it was expected. However, the application of the erosion and dilation induced by the proposed fuzzy order does not produce false colors.

Fig. 10 shows the comparison between lexicographical and fuzzy orders using the SE defined by the metric  $d_\infty$  with  $r=5$ . The upper part of Fig. 10 contains an image (a), the same image eroded with the fuzzy order (b) and the lexicographical one (c). It can be seen that when applying lexicographic order, no false colors appear but the quality of the original image is not preserved. Regarding dilation (the original image and its corresponding dilated images using fuzzy and lexicographical orders are respectively shown in (d), (e) and (f)) when lexicographical order is used the interior of the object loses its smooth coloring. However, the image after dilation when the proposed method is applied does not present these issues.

In addition, it is also interesting to check if the operators introduced in this paper represent an extension of gray level images. To make such checkup, the image authored by Heine [44] (Fig. 6 (a)) is used. Fig. 11 shows the original image (a), the erosion (b) and the dilation (c) using a SE defined by the metric  $d_\infty$  with  $r=3$ . In this case, it can be seen that the effects of the erosion and the dilation over the image were the expected ones. Looking at the region composed by gray levels, it is easy to check that the area occupied by a clear image area surrounded by dark areas tends to



**Fig. 10.** Comparison between fuzzy and lexicographic order using a synthetic image containing colored balls. (a) Original synthetic image. (b) Erosion with fuzzy order. (c) Erosion with lexicographic order. (d) Original synthetic image. (d) Dilation with fuzzy order. (f) Dilation with lexicographic order. (For interpretation of the references to color in this figure caption, the reader is referred to the web version of this paper.)



**Fig. 11.** Effects of basic operators. (a) Original image. (b) Erosion. (c) Dilation.

be reduced. Similar effects occurs for the colors whose intensity tends to decrease, resulting in a darker image. In the dilation, the gray levels for the area occupied by a clear image area surrounded by dark areas tends to expand while colorful areas tend to increase in intensity, creating a clearer image. It is important to highlight that this application does not generate false colors. This is because it does not create new combinations of values for each pixel.

The gradient information is widely used in image processing for detecting edges. In MM, there are several digital implementations of the gradient. The most used are the morphological gradient, the gradient by erosion and the gradient by dilation given in Definition 6. Fig. 12 shows the effects of these kind of operators in color images. Image (a) in Fig. 12 shows the morphological gradient computed through the subtraction between the dilation and

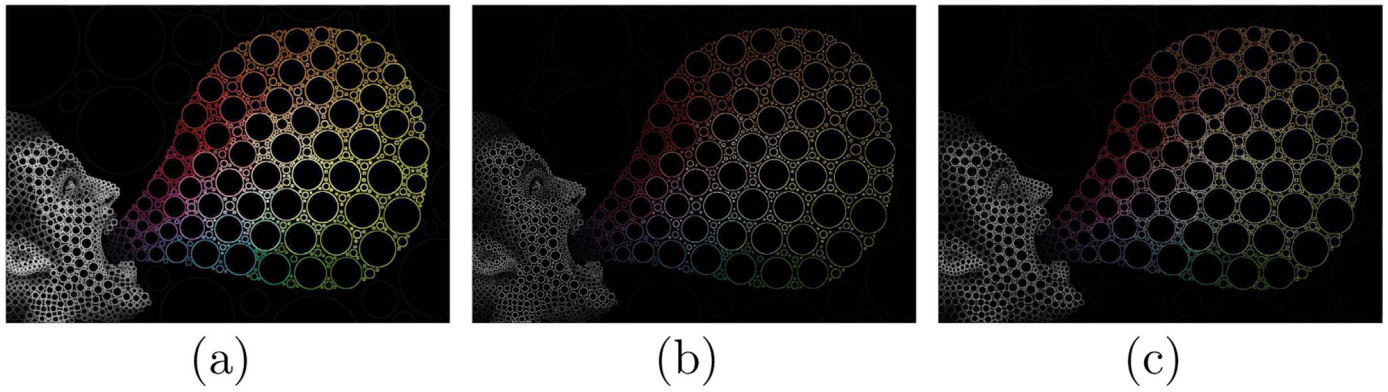


Fig. 12. Edge detection. (a) Morphological gradient. (b) Gradient by erosion. (c) Gradient by dilation.

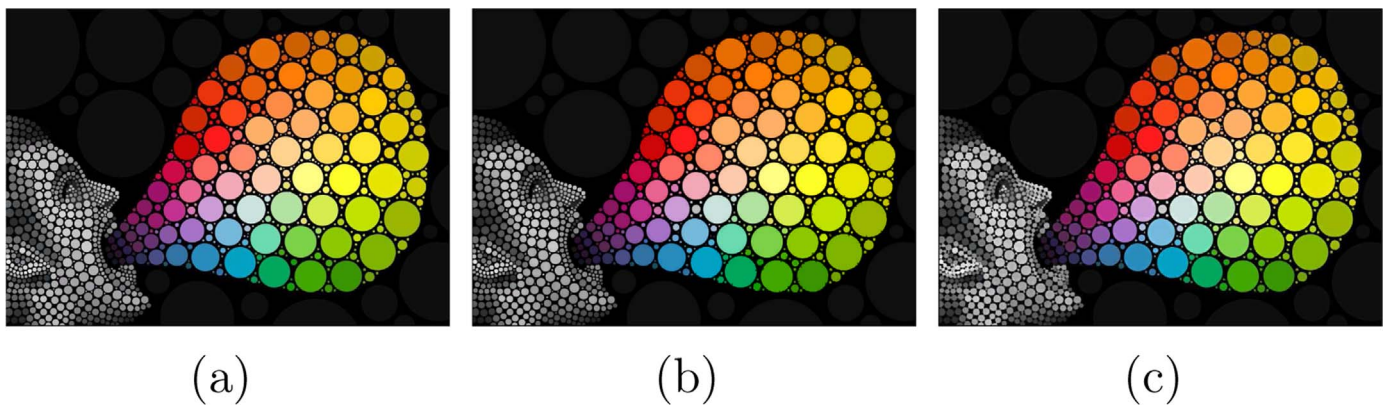


Fig. 13. Filter operators. (a) Original image. (b) Opening. (c) Closing.



Fig. 14. Example of the 68 texture of Outex13.

**Table 1**  
Classification rates in percent for textures of Outex13, using erosion based covariance.

	Order		
	Fuzzy order	M-order	Lexicographic order
RGB	77.20	77.65	70.74

the erosion. Secondly, image (b) shows the gradient by erosion obtained by the subtraction between the original image and the erosion, and finally (image (c)), the gradient by dilation is presented (obtained through the dilation minus the original image). The colors that appear in the gradients can be new colors because they were generated as a result of a vectorial subtraction. This

means that false colors are independent of the proposed order.

Finally, opening and closing basic filters (see Definition 6) are studied. The opening is defined as an erosion followed by a dilation. This filter generally smooths the outline of the image, eliminating the narrow parts and thin protrusions. It is useful for removing small bright details regarding the SE, leaving the rest of the image relatively unchanged. This effect can be seen in Fig. 13(a).

The closing, defined as a dilation followed by an erosion, also tends to smooth the contours, but unlike opening, it merges narrow spaces, and long and thin entries. In addition, it eliminates small gaps and fill spaces in the outline. It is useful to eliminate small dark details regarding the SE, leaving the rest of the image relatively unchanged. This effect can be seen in Fig. 13(b). As these operators are combinations of erosions and dilations, false colors neither appear.

As there is no obvious criteria to compare the performance of these kinds of operators, the effects produced by these operators over the image are shown. This is because there is no obvious reason for saying, for example, why the green color should be greater than the red one from the human perception point of view. In [38,45] it was explained that it is difficult to perform a quantitative comparison between morphological approaches only through the results given by their basic operations, because there is no obvious criteria to apply in order to generate which approach is better.

One of the most important features in the visual perception and description of natural images is the notion of texture. Thus, the performance of the operators introduced in this paper is now studied following the model for texture classification presented in [2]. In this model the authors use the Outex framework, which (see [46]) contains a large collection of surface textures captured under different conditions, which facilitates construction of a wide range of texture analysis problems. The image database contains an

extensive collection of textures, both in form of surface textures and natural scenes. In particular the color textures of Outex13 (see Fig. 14) are employed here.

One of the most frequent texture analysis tools offered by mathematical morphology is the so-called morphological covariance, which is introduced adopting the notations used in [2] or [47].

The morphological covariance  $K'$  of an image  $f$ , is defined as the volume  $Vol$  of the image (i.e. sum of pixel values), eroded by a pair of points  $P_{2,\nu}$  separated by a vector  $\nu$ :

$$K'(f; P_{2,\nu}) = Vol(\varepsilon_{P_{2,\nu}}(f)), \quad (18)$$

where  $\varepsilon$  denotes the erosion operator. In practice,  $K'$  is computed for varying lengths of  $\nu$ , and most often, as also here, the normalized version  $K$  is used for measurements:

$$K(f) = Vol(\varepsilon_{P_{2,\nu}}(f))/Vol(f). \quad (19)$$

The covariance based in increasing lineal SE ( $0^\circ$ ,  $45^\circ$ ,  $90^\circ$ ,  $135^\circ$ ) order from 1 to 49 pixels in steps on size two is computed. Consequently 25 values are available for each direction.

Table 1 shows the accuracy rates obtained for the erosion with fuzzy, M and lexicographic orders. Although the values for the fuzzy order and M-order are similar, when fuzzy orders are applied, false colors are not obtained.

Other authors carry out similar experiments for both Lexicographic and M-orders (see [2,43]). In fact, in Table 5 of [2] the accuracy rate for M-order is 77.65 and for lexicographic one is 70.74. These values are compared (see Table 1) to those obtained by fuzzy order under the same conditions, i.e., same image basis and considering the  $k$ -nearest neighbors (K-NN) algorithm and Euclidean distance. Unfortunately, we cannot compare our results with those of van de Gronde and Roerdink [43] because they have used a different way to apply the operators. In any case, we can observe (see Fig. 12 in page 1287) that the group-invariant frames lead to better performance than the original RGB basis (RGB: 81.8, hue: 84.1, and rotation: 85.4).

## 6. Conclusions

In this paper, basic morphological operators for color images using a fuzzy total order are introduced. That is, a fuzzy mathematical morphology for color images is presented. These operators present interesting properties. In particular, they extend gray level operators of the mathematical morphology to color image processing framework and they do not produce false colors. In addition, the suggested fuzzy order allows giving the same importance to all the components of the image, not prioritizing some of the component over the others as the lexicographic order does. Moreover, when the performance of the operators is studied in the context of texture classification, the accuracy rates obtained for the erosion with the fuzzy order are close to the ones obtained with other orders, but avoiding false colors. It is also important to highlight that the proposed operator generates a flexible method for segmentation as the OWA and aggregation functions can be tuned according to the proposed image analysis.

As future work, we plan to study the behavior of this method when other color representations are used. Besides, other orders will be analyzed in order to produce new erosion and dilation operators for color images. In addition, we will consider these operators for image segmentation. Finally, we will analyze the way to extend our method to “non-flat” mathematical morphology operators.

## References

- [1] J. Angulo, Morphological color operators in totally ordered lattices based on distances: application to image filtering, enhancement and analysis, *Comput. Vis. Image Underst.* 107 (1) (2007) 56–73.
- [2] E. Aptoula, S. Lefevre, A comparative study on multivariate mathematical morphology, *Pattern Recognit.* 40 (11) (2007) 2914–2929.
- [3] E. Aptoula, S. Lefevre, On lexicographical ordering in multivariate mathematical morphology, *Pattern Recognit. Lett.* 29 (2) (2008) 109–118.
- [4] M.C. d'Ornellas, J.A.T. Borges da Costa, Color mathematical morphology based on partial ordering of spectra, in: XX Brazilian Symposium on Computer Graphics and Image Processing, 2007, SIBGRAPI 2007, 2007, pp. 37–44.
- [5] G. Matheron, *Random Sets and Integral Geometry*, Wiley, New York, 1975.
- [6] J. Serra, *Image Analysis and Mathematical Morphology*, vol. I, Academic Press, London, 1982.
- [7] J. Serra, *Image Analysis and Mathematical Morphology*, vol. II, Academic Press, London, 1988.
- [8] C. Ronse, Why mathematical morphology needs complete lattices, *Signal Process.* 21 (2) (1990) 129–154.
- [9] J. Angulo, J. Serra, Mathematical morphology in color spaces applied to the analysis of cartographic images, in: Proceedings of GEOPRO, vol. 3, 2003, pp. 59–66.
- [10] A. Hanbury, J. Serra, Mathematical morphology in the HLS color space, in: BMVC, 2001, pp. 1–10.
- [11] A. Hanbury, J. Serra, Mathematical Morphology in the L\*a\*b\* Color Space, Centre de Morphologie Mathématique Ecole des Mines de Paris, Perancis, 2001.
- [12] A. Hanbury, J. Serra, Mathematical morphology in the CIELAB space, *Image Anal. Stereol.* 21 (3) (2002) 201–206.
- [13] P. Lambert, J. Chanussot, Extending mathematical morphology to color image processing, in: CGIP'00 – 1st International Conference on Color in Graphics and Image, 2000, pp. 158–163.
- [14] A. Ledda, W. Philips, Majority ordering for color mathematical morphology, in: Proceedings of the XIIIth European Signal Processing Conference, Antalya, Turkey, 2005.
- [15] O. Lezoray, C. Meurie, A. Elmoataz, A graph approach to color mathematical morphology, in: Proceedings of the Fifth IEEE International Symposium on Signal Processing and Information Technology, 2005, 2005, pp. 856–861.
- [16] G. Louverdis, M.I. Vardavoulia, I. Andreadis, P. Tsalides, A new approach to morphological color image processing, *Pattern Recognit.* 35 (8) (2002) 1733–1741.
- [17] A. Soria-Frisch, M. Koepfen, Fuzzy color morphology based on the fuzzy integral, in: Proceedings of the International ICSC Congress on Computational Intelligence: Methods and Applications, CIMA'2001, 2001, pp. 732–737.
- [18] J.L. Vazquez Noguera, H. Legal Ayala, C.E. Schaerer, J. Facon, A color morphological ordering method based on additive and subtractive spaces, in: 2014 IEEE International Conference on Image Processing, ICIP, 2014, pp. 674–678.
- [19] M. Wheeler, M.A. Zmuda, Processing color and complex data using mathematical morphology, in: Proceedings of the IEEE 2000 National Aerospace and Electronics Conference, 2000, NAECON 2000, 2000, pp. 618–624.
- [20] V. Barnett, The ordering of multivariate data, *J. R. Stat. Soc. Ser. A (Gen.)* (1976) 318–355.
- [21] J. Angulo, J. Serra, Morphological coding of color images by vector connected filters, in: Proceedings of the Seventh International Symposium on Signal Processing and Its Applications, 2003, vol. 1, 2003, pp. 69–72.
- [22] M.A. Veganzones, M. Dalla Mura, G. Tochon, J. Chanussot, Binary partition trees-based spectral-spatial permutation ordering, in: J.A. Benediktsson, J. Chanussot, L. Najman, H. Talbot (Eds.), *Mathematical Morphology and Its Applications to Signal and Image Processing*, Lecture Notes in Computer Science, LNCS, vol. 9082, Springer, Switzerland, 2015, pp. 434–445.
- [23] B. De Baets, E. Kerre, M. Gupta, The fundamentals of fuzzy mathematical morphology. Part 1: basic concepts, *Int. J. Gen. Syst.* 23 (2) (1995) 155–171.
- [24] B. De Baets, E. Kerre, M. Gupta, The fundamentals of fuzzy mathematical morphology. Part 2: idempotence, convexity and decomposition, *Int. J. Gen. Syst.* 23 (4) (1995) 307–322.
- [25] B. De Baets, Idempotent closing and opening operations in fuzzy mathematical morphology, in: Third International Symposium on Uncertainty Modeling and Analysis and Annual Conference of the North American Fuzzy Information Processing Society, Proceedings of ISUMA-NAFIPS'95, 1995, pp. 228–233.
- [26] I. Bloch, H. Maitre, Constructing a fuzzy mathematical morphology: alternative ways, in: Second IEEE International Conference on Fuzzy Systems, 1993, 1993, pp. 1303–1308.
- [27] I. Bloch, H. Maitre, Fuzzy mathematical morphologies: a comparative study, *Pattern Recognit.* 28 (9) (1995) 1341–1387.
- [28] I. Bloch, Duality vs. adjunction for fuzzy mathematical morphology and general form of fuzzy erosions and dilations, *Fuzzy Sets Syst.* 160 (13) (2009) 1858–1867.
- [29] V. di Gesù, M.C. Maccarone, M. Tripiciano, Mathematical morphology based on fuzzy operators, in: R.L. Owen, M. Roubens (Eds.), *Fuzzy Logic*, Kluwer Academic Publishers, Netherlands, 1993, pp. 477–486.
- [30] P. Burillo López, N. Frago Paños, R. Fuentes-González, Fuzzy morphological operators in image processing, *Mathw. Soft Comput.* 10 (2) (2003) 85–100.
- [31] S. Velasco-Forero, J. Angulo, Random projection depth for multivariate mathematical morphology, *IEEE J. Sel. Top. Signal Process.* 6 (7) (2012) 753–763.
- [32] S. Velasco-Forero, J. Angulo, Classification of hyperspectral images by tensor

- modeling and additive morphological decomposition, *Pattern Recognit.* 46 (2) (2013) 566–577.
- [33] G. Franchi, J. Angulo, Ordering on the probability simplex of endmembers for hyperspectral morphological image processing, in: J.A. Benediktsson, J. Chanussot, L. Najman, H. Talbot (Eds.), *Mathematical Morphology and Its Applications to Signal and Image Processing*, Lecture Notes in Computer Science, LNCS, vol. 9082, Springer, Switzerland, 2015, pp. 375–386.
- [34] R. González, R. Woods, *Digital Image Processing*, Addison-Wesely Publishing Company, USA, 1996.
- [35] M. Nachtgaele, E. Kerre, Connections between binary, gray scale and fuzzy mathematical morphologies, *Fuzzy Sets Syst.* 124 (1) (2001) 73–85.
- [36] M. Valle, R. Valente, Elementary morphological operations on the spherical CIE Lab quantale, in: J.A. Benediktsson, J. Chanussot, L. Najman, H. Talbot (Eds.), *Mathematical Morphology and Its Applications to Signal and Image Processing*, Lecture Notes in Computer Science, LNCS, vol. 9082, Springer, Switzerland, 2015, pp. 375–386.
- [37] A. Bouchet, P. Quirós, P. Alonso, V. Ballarin, I. Díaz, S. Montes, Gray scale edge detection using interval-valued fuzzy relations, *Int. J. Comput. Intell. Syst.* 8 (2) (2015) 16–27.
- [38] A. Căliman, M. Ivanovici, N. Richard, Probabilistic pseudo-morphology for grayscale and color images, *Pattern Recognit.* 47 (2) (2014) 721–735.
- [39] F. Chiclana, F. Herrera, E. Herrera-Viedma, Integrating three representation models in fuzzy multipurpose decision making based on fuzzy preference relations, *Fuzzy Sets Syst.* 97 (1998) 33–48.
- [40] R. Pérez-Fernández, P. Alonso, I. Díaz, S. Montes, Multi-factorial risk assessment: an approach based on fuzzy preference relations, *Fuzzy Sets Syst.* (2015), <http://dx.doi.org/10.1016/j.fss.2014.10.012>.
- [41] R.R. Yager, On ordered weighted averaging aggregation operators in multi-criteria decision making, *IEEE Trans. Syst. Man Cybern.* 18 (1988) 183–190.
- [42] X. Wang, E.E. Kerre, Reasonable properties for ordering of fuzzy quantities (ii), *Fuzzy Sets Syst.* 118 (2001) 387–405.
- [43] J.J. van de Gronde, J.B. Roerdink, Group-invariant color morphology based on frames, *IEEE Trans. Image Process.* 23 (3) (2014) 1276–1288.
- [44] B. Heine, *Image by Ben Heine* ([www.benheine.com](http://www.benheine.com)), 2015.
- [45] A. Ledoux, N. Richard, A.S. Capelle-Laizé, The fractal estimator: a validation criterion for the color mathematical morphology, in: *Conference on Color in Graphics, Imaging, and Vision*, Society for Imaging Science and Technology, Netherlands, 2012, pp. 206–210.
- [46] T. Ojala, T. Mäenpää, M. Pietikäinen, J. Viertola, J. Kyllönen, S. Huovinen, Outex: new framework for empirical evaluation of texture analysis algorithms, in: *Proceedings 16th International Conference on Pattern Recognition*, vol. 1, 2002, pp. 701–706.
- [47] E. Aptoula, S. Lefevre, Spatial morphological covariance applied to texture classification, in: B. Günsel, A.K. Jain, A.M. Tekalp, B. Sankur, Bülent (Eds.), *Multimedia Content Representation, Classification and Security: International Workshop*, Springer, Heidelberg, 2006, pp. 522–529.

**Agustina Bouchet** received her degree of Professor in Mathematics and bachelor's degree in Mathematics Sciences at Universidad Nacional de Mar del Plata (UNMdP), Mar del Plata, Argentina, in 2003 and 2005 respectively. In 2010, she received her Ph.D. degree in Engineering, Electronics Orientation. Since 2002, she works in the Group of Digital Image Processing, School of Engineering at Universidad Nacional de Mar del Plata, studying the behavior of fuzzy mathematical morphology operators and their application in biomedical image processing. Currently, she is a research assistant in the National Scientific and Technical Research (CONICET).

**Pedro Alonso** is a professor of the Department of Mathematics at the University of Oviedo, Spain. He is graduated in Mathematics and he received the M.Sc. degree in Mathematics, from the University of Oviedo in 1995 (cum laude). His main interests are in numerical linear algebra, error analysis, study of algorithms (complexity, performance, stability, convergence, etc.), high performance computing, and parallel computing. He has several publications in international journals and communications in international conferences, and he is participating in several projects at the moment.

**Juan Ignacio Pastore** received his B.Sc. in Mathematics Sciences in 2000 from the Mathematical Department at Universidad Nacional de Mar del Plata (UNMdP), Mar del Plata, Argentina and his Ph.D. in Electronics Engineering in 2009 from the Department of Electronic Engineering at the same university. He is currently a member of the Digital Image Processing Group in charge of the mathematical area of the main research project. His research interest areas include biomedical images processing, pattern recognition, mathematical morphology, among others. He is also currently a researcher of the National Scientific and Technical Research Council (CONICET), an agency of the Ministry of Science, Technology and Productive Innovation of Argentina.

**Susana Montes** received the M.Sc degree in Mathematics, Option Statistics and Operational Research, from the University of Valladolid, Spain, in 1993, and the Ph.D. degree from the University of Oviedo, Spain, in 1998 (cum laude). She received the Best Mathematics Ph.D. Thesis Award from the University of Oviedo. She is a professor of Statistics and O.R. at the University of Oviedo, where she is the leader of the research group UNIMODE. She has several publications in international journals and communications in international conferences, and she is participating in several national and international projects at the moment, some of them led by her. She is an associate editor of the *Journal of Intelligent & Fuzzy Systems* and the *Electronic Journal of Applied Statistical Analysis*.

**Irene Díaz** received the M.Sc degree in Mathematics from the University of Oviedo, Spain, in 1995, and the Ph.D. degree from the University Carlos III of Madrid, Spain, in 2001 (cum laude). She is a senior lecturer at the Computer Science Department of the University of Oviedo. She has several publications in international journals and communications in international conferences, most of them focused on data analysis.